



Influence of the ligand structure on the properties of bidentate salicylaldimine nickel(II) complexes in ethylene oligomerization

Yang Li¹ · Lijun Guo¹ · Feng Li¹ · Jin Huang^{1,2} · Dan Li¹ · Na Zhang¹ · Cuiqin Li¹

Received: 2 October 2020 / Accepted: 4 January 2021 / Published online: 2 February 2021
© The Author(s), under exclusive licence to Springer Nature Switzerland AG part of Springer Nature 2021

Abstract

Three nickel(II) complexes (**C1–C3**) bearing diamine-bridged 4-hydroxysalicylaldehyde ligands (**L1–L3**) were successfully synthesized, and all the compounds were characterized by physicochemical and spectroscopic methods. The influence of the oligomerization parameters on the catalytic properties of complex **C2** was systematically investigated. The results showed that oligomerization parameters played an important role in the catalytic properties and the catalytic activity was 19.90×10^4 g/(mol·Ni·h) and the selectivity of C_{8+} olefins was 60.25% when the precatalyst dosage was 5 μ mol, the Al/Ni molar ratio was 500, the temperature was 25 °C, the reaction time was 30 min and the pressure of ethylene was 0.7 MPa. Complexes **C1–C3** with different lengths of the bridged group were evaluated for ethylene oligomerization, and the results showed that the length of the alkyl chain in the ligand had little influence on the catalytic properties. Complex **C4** based on ethanediamine-bridged salicylaldimine and **C5** based on the hyperbranched salicylaldimine in our previous work were also investigated to study the influence of the ligand structure on the catalytic properties. The catalytic activity [31.80×10^4 g/(mol·Ni·h)] and the content of the low-carbon oligomers (70.16%) for complex **C4** were higher than complex **C2** with hydroxyl substituent in benzene ring. The catalytic activity and the content of the low carbon oligomers for complex **C5** were far higher than other four complexes.

Introduction

The discovery of cationic Ni(II) and Pd(II) precatalysts by Brookhart triggered a true exploration of the late-transition metal precatalysts for olefin polymerization [1, 2]. Compared to early-transition metal precatalysts, the nickel(II) precatalysts had a higher tolerance toward the polar reagents and offered the potential to yield polymers with different microstructures and properties [3]. Great progress had been made in the area of ethylene polymerization with

late-transition metal complexes, particularly the nickel complexes, as precatalysts over the last 2 decades [4, 5]. Saad et al. [6] synthesized first-generation and second-generation pyridylimine-terminated nickel dihalide metallodendrimers, and these metallodendrimers were applied to the ethylene oligomerization. The results showed that the nickel complexes exhibited the promising catalytic activities and the polymerization products contained low-density polyethylene with the branching structure and high-density polyethylene with the linear chain structures.

At the beginning of the century, the discovery of salicylaldimine catalysts synthesized by Grubbs was another breakthrough facilitating forays into neutral nickel catalysts [7, 8]. More and more investigations have focused on the improvement in the catalytic properties through modification of the precatalyst structure [9, 10]. For the past few years, our group has been absorbed in the research focused on late-transition metal precatalysts based on salicylaldimine Schiff base ligands with various structures. Chen and her co-workers synthesized a series of nickel complexes with 3-substituted salicylaldehyde-imine ligands based on ethylenediamine and explored the influence of the electronic and steric effect of the ligands on catalytic properties of nickel

Supplementary material The online version contains supplementary material available at (<https://doi.org/10.1007/s11243-021-00447-7>).

✉ Cuiqin Li
dqpicuiqin@126.com

- ¹ Heilongjiang Provincial Key Laboratory of Oil and Gas Chemical Technology, College of Chemistry and Engineering, Northeast Petroleum University, Daqing 163318, Heilongjiang, China
- ² Heilongjiang Provincial Key Laboratory of Oilfield Applied Chemistry and Technology, Daqing Normal University, Daqing 163712, Heilongjiang, China

complexes in ethylene oligomerization [11]. Compared with the complexes with the tert-butyl group and the methoxy group, the nickel complex with methyl group performed the highest activity of 1.63×10^6 g/(mol·Ni·h) in ethylene oligomerization and showed the specific selectivity toward C₈–C₁₂ olefin. Wang and co-workers synthesized a series of nickel complexes based on hyperbranched salicylaldimine ligands and explored the relationship between the structure of salicylaldimine ligands and the catalytic activity [12]. The results showed that the catalytic activity decreased with the increase in molecular cavity. The complexes with the smaller molecular cavity displayed a higher catalytic activity [5.80×10^5 g/(mol·Ni·h)] and a high carbon olefin content (16.25%).

A majority of the investigations on nickel precatalysts have focused on the benzene ring of salicylaldiminato ligands because of the facility for introducing various substituents to enhance the activity and to control the polymer microstructure. There have been a relatively small number of studies about the relationship between the alkyl chain length of the ligand backbone and the catalytic properties [13–15]. Based on the previous works, three nickel complexes based on diamine-bridged 4-hydroxysalicylaldehyde Schiff base ligands with the same substituent group of the benzene ring but the different bridged groups were synthesized to study the structure–activity relationship of these nickel complexes in ethylene oligomerization. The effects of the ligands with different steric and electronic groups on the catalytic properties were explored.

Experimental section

Materials and methods

All reactions were carried out under an atmosphere of nitrogen using standard Schlenk techniques. Solvent was dried and distilled under nitrogen prior to use. All the raw materials were purchased from Tianjin Kemiou Chemical Reagent Co. Ltd. and used without further purification. Methylaluminoxane (MAO, 10 wt% in toluene) was purchased from Sigma-Aldrich (China) and stored in N₂ atmosphere.

FTIR spectra were recorded on Bruker Vector 22 spectrophotometer in KBr pellets from 4000 to 500 cm⁻¹. ¹H NMR spectra were recorded with Bruker-400 MHz NMR in CDCl₃ with tetramethylsilane (TMS) as an internal reference. TG analyses were carried out using a thermal gravimetric analysis instrument (Diamond TG/DTA Perkin-Elmer SII) with a flow rate of 20 mL/min and the range of 25–850 °C with the heating rate of 10 °C/min. The element analysis of the nickel complexes was calculated using ICPS-7510 spectrometer. The detail process was as follows: the samples were prepared by treating 15 mg of

the nickel complex with 2 mL of HCl, 6 mL of HNO₃ and 5 mL of HF, adding the mixture to Teflon autoclaves and subsequently using a digester for 24 h at 120 °C. After cooling to room temperature, the samples were diluted to 50 mL with deionized water. GC analyses of oligomers were performed on a Fuli GC9720 equipped with a flame ionization detector (FID) and a 50 μm (0.2 mm i.d., 0.5 μm film thickness) HP-PONA column. PXRD analysis was performed using X-ray diffraction of Japan (CuK alpha radiation, tube voltage 40 kV, tube current 30 mA, scan rate 10°/min, scanning scope 2θ = 10°–80°).

Synthesis of series of diamine-bridged 4-hydroxysalicylaldehyde ligands (L1–L3)

Under nitrogen atmosphere, 4-hydroxysalicylaldehyde (0.56 g, 4 mmol) and ethanediamine (0.12 g, 2 mmol) were dissolved in 20 mL ethanol, respectively. The 4-hydroxysalicylaldehyde solution was added to the ethanediamine solution drop by drop. The reaction mixture was refluxed for 6 h, and a light-yellow precipitate was obtained. Then, the precipitate was separated by filtration and washed with ethanol. The solid was dried in vacuum at 80 °C for 24 h to obtain the ethylenediamine-bridged 4-hydroxysalicylaldehyde imine ligand (L1) based on ethylenediamine as a light-yellow solid, and the yield was 94%. Anal. Calcd. for C₁₆H₁₆N₂O₄ (300): C 64.00, H 5.33, N 9.34. Found: C 64.05, H 5.41, N 9.37. IR data (KBr cm⁻¹): ν(C=N) 1642 and ν(C–O) 1236. ¹H NMR (400 MHz, CDCl₃) δ 8.15 (2H, –CH=N–), 6.07–7.06 (6H, Ph-H), 4.89 (4H, Ph-OH), 3.84 (4H, –CH₂–N=C–).

The 4-hydroxysalicylaldehyde imine ligand (L2) based on butanediamine was prepared with the same synthetic method as L1 using 4-hydroxysalicylaldehyde (0.56 g, 4 mmol) and butanediamine (0.18 g, 2 mmol) as materials. Light-yellow solid was obtained and the yield was 93%. Anal. Calcd. for C₁₈H₂₀N₂O₄ (328): C 65.85, H 6.09, N 8.54. Found: C 65.81, H 6.05, N 8.57. IR data (KBr cm⁻¹): ν(C=N) 1646 and ν(C–O) 1226. ¹H NMR (400 MHz, CDCl₃) δ 8.12 (2H, –CH=N–), 6.12–7.07 (6H, Ph-H), 4.92 (4H, Ph-OH), 3.33 (4H, –CH₂–N=C–), 1.75 (4H, –CH₂–C–N=C–).

The 4-hydroxysalicylaldehyde imine ligand (L3) based on hexamethylenediamine was prepared with the same synthetic method as L1 using 4-hydroxysalicylaldehyde (0.56 g, 4 mmol) and hexamethylenediamine (0.23 g, 2 mmol) as materials. Light-yellow solid was obtained and the yield was 92%. Anal. Calcd. for C₂₀H₂₄N₂O₄ (356): C 67.42, H 6.74, N 7.87. Found: C 67.51, H 6.79, N 7.817. IR data (KBr cm⁻¹): ν(C=N) 1643 and ν(C–O) 1232. ¹H NMR (400 MHz, CDCl₃) δ 8.08 (2H, –CH=N–), 6.11–7.04 (6H, Ph-H), 4.88

(s, 4H, O–H), 3.58 (4H, –CH₂–N=C–), 1.54–1.39 (4H, –CH₂–C–N=C–), 1.16 (4H, –CH₂–C–C–N=C–).

Synthesis of series of bidentate salicylaldehyde imine nickel complexes (C1–C3)

L1 (0.30 g, 1 mmol) and nickel acetate tetrahydrate (0.25 g, 1 mmol) were dissolved in 40 mL ethanol under nitrogen atmosphere. The reaction mixture was stirred for 12 h at 78 °C under nitrogen atmosphere and the khaki solid formed. The olive khaki powder was collected by filtration and washed with ethanol. The solid was dried in vacuum at 80 °C for 24 h to obtain the 4-hydroxysalicylaldehyde imine nickel (**C1**) based on ethanediamine, and the yield was 83%. FTIR data (KBr cm⁻¹): $\nu(\text{C}=\text{N})$ 1621 and $\nu(\text{C}-\text{O})$ 1232. Anal. calcd for C₁₆H₁₄O₄N₂Ni (357): C 53.78, H 3.92, N 7.84. Found: C 53.52, H 3.74, N 7.87. Anal. by ICP (atomic %): Ni 16.53 (Calcd.), 16.65 (Found). MS (m/z): 299.1 [M–Ni]⁺, 179.1 [M–Ni–C₆H₆O₂]⁺.

The 4-hydroxysalicylaldehyde imine nickel (**C2**) based on butanediamine was prepared using the same synthetic method as **C1** with **L2** (0.33 g, 1 mmol) and nickel acetate tetrahydrate (0.25 g, 1 mmol) as materials. The khaki powder was obtained and the yield was 84%. IR data (KBr cm⁻¹): $\nu(\text{C}=\text{N})$ 1624 and $\nu(\text{C}-\text{O})$ 1222. Anal. calcd for C₁₈H₁₈O₄N₂Ni (385): C 56.11, H 4.68, N 7.27. Found: C 56.03, H 4.61, N 7.19. Anal. by ICP (atomic %): Ni 15.32 (Calcd.), 15.43 (Found). MS (m/z): 348.3 [M–2OH]⁺, 325.3 [M–Ni]⁺, 292.2 [M–Ni–2OH]⁺.

The 4-hydroxysalicylaldehyde imine nickel (**C3**) based on hexamethylenediamine was prepared using the same synthetic method as **C1** with **L3** (0.36 g, 1 mmol) and nickel acetate tetrahydrate (0.25 g, 1 mmol) as materials. The khaki powder was obtained and the yield was 84%. IR data (KBr cm⁻¹): $\nu(\text{C}=\text{N})$ 1606 and $\nu(\text{C}-\text{O})$ 1224. Anal. calcd for C₂₀H₂₂O₄N₂Ni (413): C 58.11, H 5.33, N 6.78. Found: C 58.03, H 5.25, N 6.70. Anal. by ICP (atomic %): Ni 14.29 (Calcd.), 14.36 (Found). MS (m/z): 353.1 [M–Ni]⁺, 320.6[M–Ni–2OH]⁺.

Ethylene oligomerization

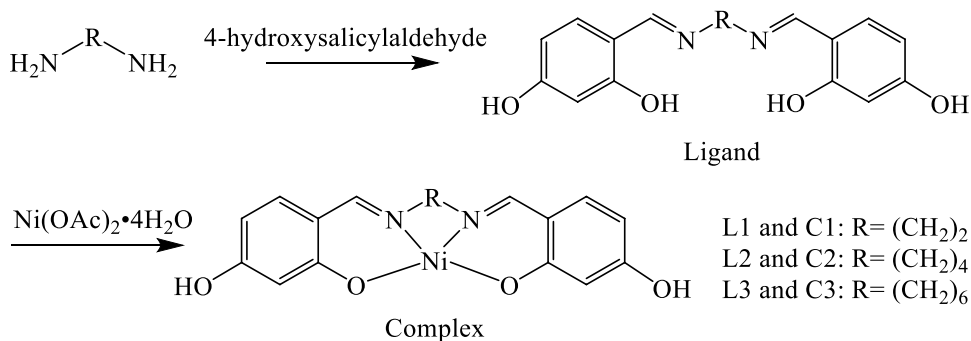
Ethylene oligomerization was carried out in a 100-ml stainless steel autoclave equipped with a magnetic stirrer and ethylene pressure control system. The reactor was charged with ethylene three times under vacuum. Under ethylene atmosphere, the appropriate amounts of solvent, cocatalyst and precatalyst precursor were injected into the reactor with a syringe, respectively. Ethylene must be supplied continuously in order to hold the desired stable pressure. The mixture was vigorously stirred for the desired time under the appropriate pressure of ethylene throughout the experiment. After the reaction, the reaction mixture was cooled in an ice-water bath and the gas mixture was collected with gas bags. The liquid mixture was quenched by 10% hydrochloric acid in ethanol. The qualitative analysis of gas mixture and the liquid mixture was identified by GC. The chromatographic analyses were performed on a Fuli GC9720 instrument equipped with HP-PONA capillary column (60 m long, 0.25 mm ID, 0.5 μm film thickness). The analysis conditions were 50 °C for 5 min, heated at 10 °C/min until the temperature reached 140 °C, then heated at 5 °C/min until the temperature reached 240 °C and maintained at the temperature for 5 min. The oligomers were identified by co-injecting n-hexane as the internal standard for quantification.

Results and discussion

Synthesis and characterization of bidentate nickel complexes

A series of diamine-bridged 4-hydroxysalicylaldehyde ligands and their nickel complexes were synthesized with the method described in the literature [16], and the products were all formed in high yield. The synthesis routes of the ligands and their nickel complexes are shown in Scheme 1. In these reactions, the 4-hydroxysalicylaldehyde and nickel acetate tetrahydrate were used in excess to obtain the ligands and nickel complexes with high yield. The unreacted reactants were removed by diethyl ether, and recrystallization

Scheme 1: Synthesis route of diamine-bridged Schiff ligands and their nickel complexes



was an essential step in order to improve the product purity. The nickel complexes (**C1–C3**) with the four coordinate square planar structure they were all khaki powders [17]. In order to verify the purity of the ligands and the complexes, the element content of all the complexes was measured with an element analyzer and ICPS-7510 spectrometer and the results were listed in Experimental section. The measured values of the elements were consistent with the theory chemical structure for the ligands (**L1–L3**) and the corresponding complexes (**C1–C3**). Moreover, the series of ligands and their corresponding complexes were also characterized by various analytical techniques.

Series of 4-hydroxysalicylaldehyde imine ligands (**L1–L3**) based on diamine were characterized by FTIR, ^1H NMR and PXRD. IR spectra of the ligands **L1–L3** and the complexes **C1–C3** are shown in Fig. S1. For the ligands [Fig. S1 (a)], the absorption peaks around 1645 cm^{-1} were assigned to the stretching vibration of C=N and the peaks at around 1230 cm^{-1} were associated with the stretching vibration of C–O, which indicated the successful Schiff base reaction between diamine and 4-hydroxysalicylaldehyde [18]. Compared with the FTIR spectra of the ligands, the ν (C=N) band in the IR spectra of complexes **C1–C3** [Fig. S1(b)] shifted from around 1645 cm^{-1} to 1620 cm^{-1} , and the ν (C–O) band shifted from around 1230 cm^{-1} to 1225 cm^{-1} . Moreover, the absorption peaks at 620 cm^{-1} were attributed to the stretching vibration of N–Ni in the IR spectra of complexes **C1–C3**. These results indicated an effective coordination interaction between the metal and the nitrogen and oxygen donor sites [3].

^1H NMR spectra of ligands **L1–L3** showed the azomethine proton ($-\text{CH}=\text{N}$) resonance as a sharp singlet was at around 8.15 ppm (Fig. S2), which indicated series of diamines had reacted with 4-hydroxysalicylaldehyde to form the Schiff base ligands [19]. Signals for the protons of methylenes of the alkyl chains were found in the range of 1.49–3.32 ppm, the protons of hydroxyl occurred at around 4.9 ppm and proton peaks from 7.07 to 6.12 ppm were assigned to the benzene rings. The appearance of the above characteristic proton peaks indicated that the structures of ligand were consistent with the theoretical structure.

In order to obtain the crystal structure of series of the synthesized ligands and the corresponding complexes, the single crystals were cultivated by volatilization method, diffusion method and temperature difference method, respectively. However, crystals suitable for single-crystal X-ray crystallography could not be obtained. The PXRD patterns of the ligands **L1–L3** and the nickel complexes **C1–C3** showed that they all had a certain crystal structure (Fig. S3). The PXRD patterns of the ligands showed that **L2** and **L3** had the similar crystal structures and were different from **L1**. The PXRD patterns of the complexes showed that **C2** and **C3** also had the similar crystal structures and were different

from **C1**, which might be caused by the bending and winding of flexible alkyl chains in backbones. With increase in the flexibility for the molecule of the complexes, the crystallinity decreased [20]. The PXRD patterns of the complexes [Fig. S3 (b)] showed that **C1** had the strong diffraction peaks of nickel appear at $2\theta = 19^\circ$ and 21° , respectively, which corresponded to the crystal planes (JCPDS 89-5881) of (111) and (JCPDS 89-7101) (200) of Ni–O. The nickel complexes had showed strong diffraction peaks of nickel at $2\theta = 34^\circ$ and 60° . These diffraction peaks corresponded to the crystal planes (JCPDS 78-0643) of (111) and (200) of Ni–O. Moreover, the PXRD patterns of the ligands were different from those of the corresponding complexes, which indicated that the complexes were formed by the coordination reaction between the ligands and nickel acetate tetrahydrate.

The MS spectra of the complexes **C1–C3** are shown in Fig. 1. The molecular ion peaks $[\text{M}-1]^+$ of complex **C1**, complex **C2** and complex **C3** were at 356.0, 384.2 and 412.1, respectively. The other detail peaks of MS spectra for series of 4-hydroxysalicylaldehyde imine nickel based on diamine were summarized in the synthesis section.

The TG curves of the three nickel complexes from 30 to 900°C are shown in Fig. 2. The TG curve displayed that the thermal decomposition of the complexes occurred in three stages and the three complexes had the same trend of weightlessness. The first weight loss occurred in the range of $30\text{--}150^\circ\text{C}$, and the loss values of the three complexes were 7.39%, 9.02% and 5.41%, respectively, which was attributed to the emitting of the surface and inherent moisture [21]. The second weight loss occurred in the range of $150\text{--}450^\circ\text{C}$, and the loss values of **C1–C3** were 27.31%, 42.05% and 31.37%, respectively. This significant weight loss corresponded to step-by-step oxidation and decomposition of the alkyl chain in the ligand [3]. The third weight loss occurred in the range

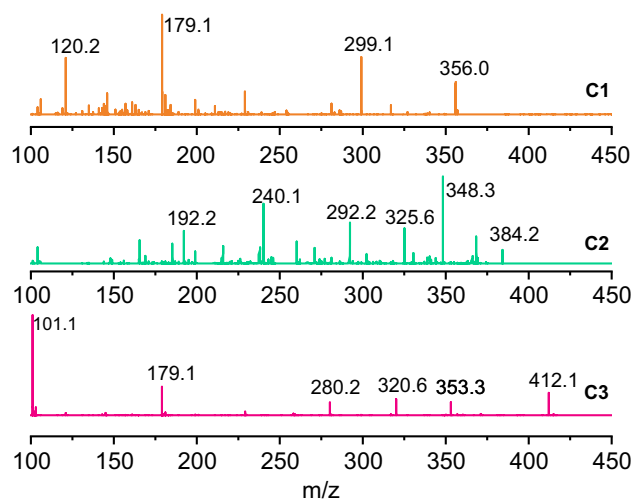


Fig. 1 MS spectra of series of nickel complexes

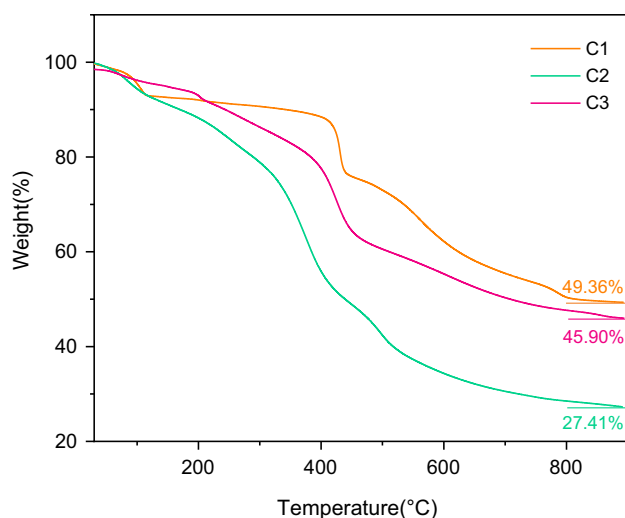


Fig. 2 TG curve of series of nickel complexes

of 450 °C to 890 °C, which corresponded to the decomposition of benzene ring in the ligand, and the weight loss values for three complexes were 15.94%, 21.52% and 17.32%, respectively. And there was no further weight loss when the temperature was above 890 °C. The results of the thermal analysis revealed that the three nickel complexes were stable up to around 150 °C.

Influence of catalytic parameters on the catalytic properties in ethylene oligomerization

The chemical structure of ligands and the oligomerization parameters had an important influence on the catalytic properties of salicylaldehyde nickel complexes in our

previous works. Because complexes **C1–C3** have similar chemical structures and the length of the bridged group for complex **C2** was between complex **C1** and complex **C3**, complex **C2** systematically investigated the changes in catalytic properties under different condition parameters in ethylene oligomerization, and the results are listed in Table 1. With increase in the precatalyst dosage at the range of 1–10 μmol , the catalytic activity increased (Entries 1–4 in Table 1), and the catalytic activity was up to the highest of $15.50 \times 10^4 \text{ g}/(\text{mol}\cdot\text{Ni}\cdot\text{h})$. This might be because more catalysts could be activated at the Al/Ni molar ratio of 500. However, with increase in the precatalyst dosage, the selectivities of C_8 and C_{10+} olefins increased firstly and reached up to 63.94% when the precatalyst dosage was 5 μmol . With further increase in the precatalyst dosage, the selectivity of C_8 and C_{10+} olefins decreased. Excess catalyst might hinder the contact of active species with ethylene, decreasing the selectivity of the high olefins [22]. Based on the catalytic activity and the selectivity of C_8 and C_{10+} olefins, the optimum precatalyst dosage was 5 μmol .

The amount of cocatalyst was found to have a great influence on the catalytic behavior of **C2/MAO** catalytic system. With an increase in the Al/Ni molar ratio from 300 to 900, the catalytic activity was sustainable growth (Entries 3 and 5–7 in Table 1). The highest activity was observed at the Al/Ni molar ratio of 900 with the value of $17.36 \times 10^4 \text{ g}/(\text{mol}\cdot\text{Ni}\cdot\text{h})$. This was because the appropriate amount of MAO might eliminate the impurities and water in solvent and might activate the nickel complex. With increase in the Al/Ni molar ratio, the content of C_8 and C_{10+} oligomers reduced, which is attributed to the high chain termination or the high chain transfer to

Table 1 Ethylene oligomerization data for **C2** catalyst systems

Entry	Precat	Dosage (μmol)	Al/Ni	Press (MPa)	Temp ($^{\circ}\text{C}$)	Activity ($10^4 \text{ g}/(\text{mol}\cdot\text{Ni}\cdot\text{h})$)	Oligomer distribution (%)			
							C_4	C_6	C_8	C_{10+}
1	C2	1	500	0.5	25	3.6	7.06	32.71	20.17	40.06
2	C2	2	500	0.5	25	8.00	5.02	34.66	24.18	36.14
3	C2	5	500	0.5	25	11.80	10.13	25.93	29.64	34.30
4	C2	10	500	0.5	25	15.50	15.01	30.32	27.08	27.62
5	C2	5	300	0.5	25	5.91	7.98	27.07	30.12	34.83
6	C2	5	700	0.5	25	14.50	21.02	39.66	24.18	15.14
7	C2	5	900	0.5	25	17.36	24.57	43.76	20.84	10.83
8	C2	5	500	0.3	25	7.69	14.45	30.52	22.12	32.91
9	C2	5	500	0.7	25	19.90	11.58	28.17	30.57	29.68
10	C2	5	500	1.0	25	21.05	12.15	27.84	31.07	28.94
11	C2	5	500	0.7	15	10.85	13.33	23.52	31.30	31.85
12	C2	5	500	0.7	35	16.68	18.29	39.26	31.51	10.94
13	C2	5	500	0.7	45	13.91	25.09	42.90	25.28	6.73

alkylaluminum by large excess of MAO [23]. Under the condition of the Al/Ni molar ratio being 500, complex **C2** had the relatively high activity [11.80×10^4 g/(mol·Ni·h)] with better selectivity for C_8 and C_{10+} oligomers (63.94%).

With increase in the reaction pressure from 0.3 to 1.0 MPa, the catalytic activity was gradually increased (Entries 3 and 8–10 in Table 1). The ethylene concentration dissolved in the catalytic system increased, which could cause more ethylene to insert into the quantitative active center, and the catalytic activity of the precatalyst increased [4]. It was worth noting that the ethylene pressure also significantly influenced the oligomer distributions. The content of C_8 and C_{10+} olefins increased firstly and then reduced slightly with the increase in the ethylene pressure, and the content of C_{8+} olefin reached up to a maximum (63.94%) when the ethylene pressure was 0.5 MPa. This might be due to the fact that the chain growth rate was greater than the chain termination rate, and it was more likely to form the high carbon olefins [11]. When the ethylene pressure was 0.7 MPa, complex **C2** had a relatively high catalytic activity [19.90×10^4 g/(mol·Ni·h)], which was far higher than the catalytic activity [11.80×10^4 g/(mol·Ni·h)] at the ethylene pressure of 0.5 MPa. At the same time, complex **C2** had relatively better selectivity of C_8 and C_{10+} oligomers (61.25%) at the ethylene pressure of 0.7 MPa. Therefore, the ethylene pressure of 0.7 MPa was the ethylene pressure of the following ethylene oligomerization.

The reaction temperature significantly affects not only the catalytic activity, but also the stability of the active species in the reaction system. The influence of the reaction temperature on the catalytic properties of complex **C2** is listed in Table 1 (Entries 9 and 11–13), and complex **C2** exhibited the highest catalytic activity at 25 °C over the range of 15–45 °C. This was because the high temperature was beneficial for the acceleration of the overall chain growth rate and the termination rate to make the increase in the catalytic activity. However, the high temperature might lead to the deactivation of the cocatalyst, and the catalytic activity decreased [24]. The selectivity of C_8 and C_{10+} oligomers decreased with the increase in the reaction temperature, which indicated that the chain termination rate increased

more rapidly than chain growth rate. Complex **C2** gave a high activity [19.90×10^4 g/(mol·Ni·h)] with better selectivity for C_8 and C_{10+} oligomers (61.25%) at 25 °C. Therefore, the reaction temperature of 25 °C was the reaction temperature of the following ethylene oligomerization.

Influence of the ligand structure on the catalytic properties in ethylene oligomerization

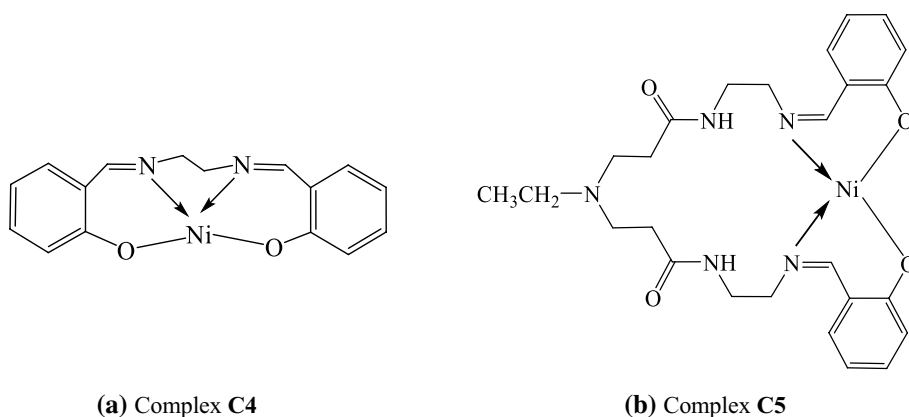
Generally, as the length of the alkyl chain in the ligand increased, the solubility of nickel complexes increased, which caused the increase in the catalytic activity [23]. In order to study the influence of the length of the alkyl chain in the ligand on the catalytic properties in ethylene oligomerization, the catalytic properties of complexes **C1–C3** were investigated when the precatalyst dosage was 5 μ mol, the Al/Ni molar ratio was 500, the temperature was 25 °C, the reaction time was 30 min and the pressure of ethylene was 0.7 MPa. And the results are listed in Table 2 (Entries 1–3). For complexes **C1–C3**, the oligomerization products had a wide distribution, and it was dominated by the products of trimerization and tetramerization of ethylene (Entries 1–3 in Table 2). With increase in the length of the alkyl chain in the ligand backbone, the catalytic activity decreased slightly and the content of C_{8+} oligomers increased slightly, which indicated that the length of the alkyl chain in the ligand had little influence on the catalytic properties. This was because the increase in the alkyl chain in the ligands caused the increase in the solubility of the nickel complexes in the reaction system, but the steric hindrance of the longer alkyl chain in the ligands resulted in the decrease in catalytic activities [11].

Complex **C4** based on ethanediamine-bridged salicylaldimine [25] and complex **C5** based on the hyperbranched salicylaldimine were evaluated [26] (Fig. 3) as precatalysts in ethylene oligomerization to study the influence of the ligand chemical structure on the catalytic properties. Compared with complex **C1**, complex **C4** had a similar structure with different substituents. There was a hydroxyl group at the fourth position that replaced the hydrogen on the benzene ring in complex **C1**. The participation of hydroxyl group led to a larger steric hindrance and the high electron density. It was the primary reason that **C1** had a lower catalyst activity

Table 2 Catalytic properties of series of nickel(II) complexes with different structures of the ligand

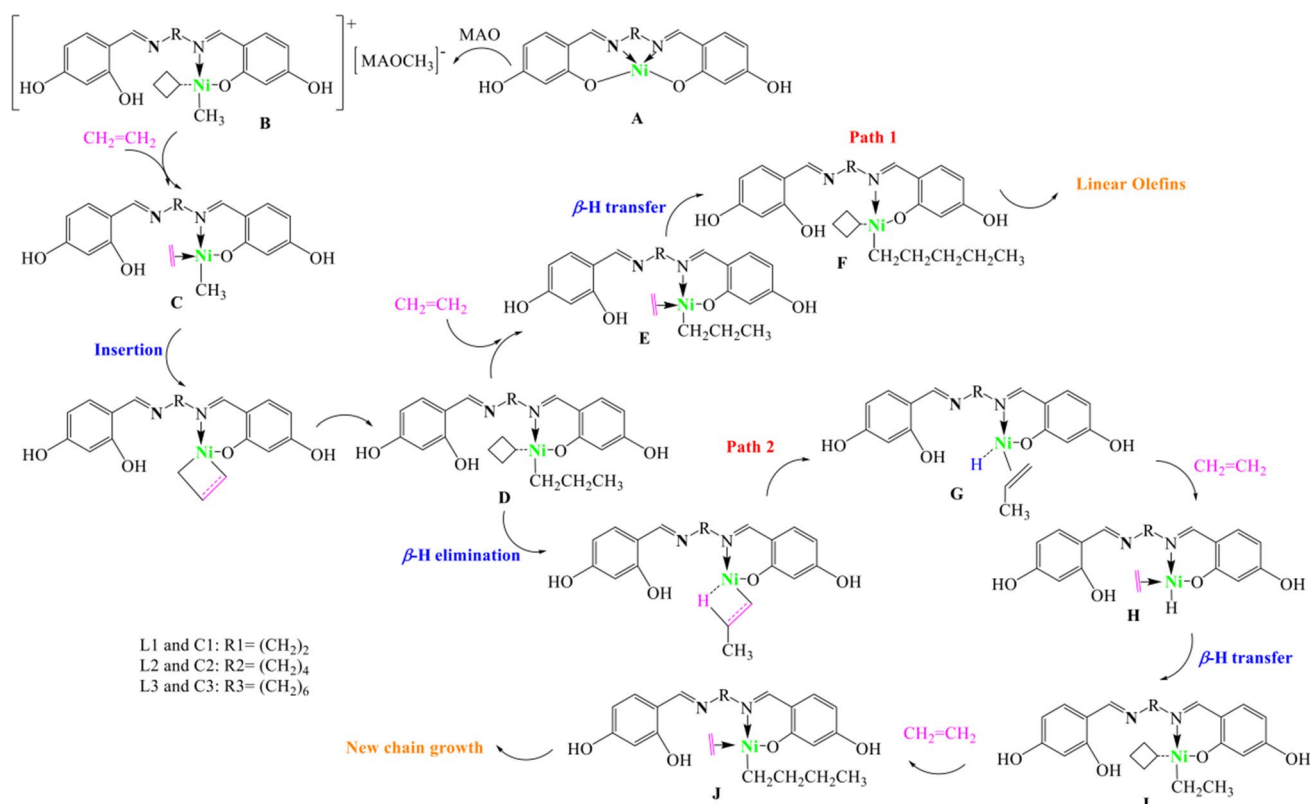
Entry	Pecat	Activity 10^4 g/(mol·Ni·h)	Oligomer distribution (%)				
			C_4	C_6	C_8	C_{10+}	Polymer
1	C1	20.12	12.76	30.12	28.96	28.16	–
2	C2	19.90	11.58	28.17	30.57	29.68	–
3	C3	18.69	11.26	26.23	31.62	30.87	–
4	C4	31.8	41.54	28.62	12.17	12.31	5.36
5	C5	112.5	87.61	8.37	2.55	1.47	–

Fig. 3 Structures of nickel(II) complexes used for ethylene oligomerization in our previous works



than **C4**. The formation of the high carbon oligomer was favored by the low steric hindrance, and polyethylene was found in the products of **C4** [11]. Compared with the other complexes, the catalytic activity and the selectivity of low carbon olefin for catalyst **C5** based on the hyperbranched salicylaldehyde ligand were much higher, which were attributed to the better solubility in the reaction system. However, the product selectivity was affected by steric and electron structure of the active center, which caused a lower chain growth rate than the chain termination rate, and the main oligomer was C_4 olefin (72.19%).

Ethylene oligomerization occurred via a plausible chain growth and termination mechanism. β -H elimination of the corresponding intermediate was critical for the formation of α -olefins [27]. The proposed mechanism of ethylene oligomerization (Scheme 2) included the initiation step: the methyl cation (**B**) formed by the reaction between diamine 4-hydroxysalicylaldehyde metal complex **A** and MAO and the complex **C** formed by interacting with an ethylene molecule into complex **B**. A second ethylene molecule is migratory insertion the metal-alkyl and formation of a new alkyl complex **D**. Ethylene could bind to this species giving the



Scheme 2: Reaction mechanism for ethylene oligomerization by diamine-bridged salicylaldehyde nickel complexes

complex E, and further insertion of ethylene lead to chain growth and the formation of linear olefins (Path 1). Alternatively, the 1-alkene hydride complex G was obtained by the β -H elimination of complex D. Further coordination between complex G and ethylene could lead to give H (Path 2), with chain transfer; a chain was terminated with the formation of a terminal olefin and a new chain was initiated [28, 29].

Conclusions

A series of diamine-bridged 4-hydroxysalicylaldehyde nickel complexes with different lengths of bridged group in ligand backbone have been synthesized and characterized. These complexes were applied as precatalysts in ethylene oligomerization to study the relationship between alkyl chain length of the ligands and catalytic properties. The oligomerization parameters had a great influence on the catalytic properties of complex **C2**. The higher pressure and the higher Al/Ni molar ratio contributed to the higher catalytic activity. The selectivity of C_{8+} olefins and the catalytic activity of complex **C2** were 60.25% and 19.90×10^4 g/(mol·Ni·h), respectively, when the Al/Ni molar ratio was 500 and the ethylene pressure was 0.7 MPa. The catalytic activities of the synthesized nickel complexes were little changed with the increase in alkyl chain length in the ligand backbone. However, the chemical structure of the ligands had an important role in the catalytic properties of nickel complexes for ethylene oligomerization. The catalytic activity [31.80×10^4 g/(mol·Ni·h)] and the content of low carbon oligomers (70.16%) for complex **C4** based on ethanediamine-bridged salicylaldehyde with a low steric hindrance were higher than complex **C1** with the similar structure. The long alkyl chain and the electron-withdrawing group in the bridged group of complex **C5** based on the hyperbranched salicylaldehyde caused the higher catalytic activity and the higher content of the low carbon olefin. Further works are in progress in order to obtain new high-performance oligomerization catalysts based on various diamine-bridged 4-hydroxysalicylaldehyde nickel complexes modulating catalytic activity and high-carbon selectivity by the length of alkyl chain in the ligand backbone.

Acknowledgements This work was supported by the Heilongjiang Natural Science Foundation of China (E2018012) for the financial support. We are grateful to State Key Laboratory of Inorganic Synthesis and Preparative Chemistry of Jilin University and Analysis and Test Center of Northeast Petroleum University for the characterization work.

References

1. Song DP, Shi XC, Wang YX, Yang JX, Li YS (2012) *Organometallics* 31:966–975
2. Johnson LK, Killian CM, Brookhart M (1995) *J Am Chem Soc* 117:6414–6415
3. Li CQ, Wang FF, Lin ZY, Zhang N, Wang J (2017) *Appl Organomet Chem* 31:e3756
4. Sun WH, Song SJ, Li BX, Redshaw C, Hao X, Li YS, Wang FS (2012) *Dalton Trans* 41:11999–12010
5. Rhinehart JL, Mitchell NE, Long BK (2014) *ACS Catal* 4:2501–2504
6. Ahamad T, Alshehri SM (2014) *Polym Int* 63:1965–1973
7. Wang CM, Friedrich S, Younkin TR, Li RT, Day MW (1998) *Organometallics* 17:3149–3151
8. Younkin TR, Connor EF, Henderson JI, Friedrich SK, Bansleben DA (2000) *Science* 287:460–462
9. Bouleus P, Lutz M, Jeanneau E, Olivier-Bourbigou H, Breuil PI (2014) *Eur J Inorg Chem* 2014:3754–3762
10. Liu H, Zhao WZ, Hao X (2011) Redshaw Carl, Sun WH. *Organometallics* 30:2418–2424
11. Chen L, Huo HL, Wang LB, Ma LL, Jiang Y, Xie JY, Wang J (2018) *Chem Res Chin Univ* 34:945–951
12. Wang J, Zhang N, Li CQ, Shi WG, Lin ZY (2016) *J Organomet Chem* 822:104–111
13. Mu HL, Ye WP, Song DP, Li YS (2010) *Organometallics* 29:6282–6290
14. Song DP, Li YG, Lu R, Hu NH, Li YS (2008) *Appl Organomet Chem* 22:333–340
15. Kim I, Kwak CH, Kim JS, Ha CS (2005) *Appl Catal A* 287:98–107
16. Bazarganipour M, Salavati-Niasari M (2016) *Chem Eng J* 286:259–265
17. Haghverdi M, Tadjarodi A, Bahri-Laleh N, Nekoomanesh-Haghighi M (2018) *Appl Organomet Chem* 32:e4015
18. Wang J, Liu JY, Chen LD, Lan TY, Wang LB (2020) *J Chem Res* 44:206–211
19. Chen R, Bacsá J, Mapolie SF (2002) *Inorg Chem Commun* 5:724–726
20. Ahmadjo S, Arabi H, Zohuri G, Nekoomanesh M, Nejabat G (2014) *J Therm Anal Calorim* 116:417–426
21. Zhang N, Wang SH, Song L, Li CQ, Wang J (2016) *Inorg Chim Acta* 453:369–375
22. Do LH, Labinger JA, Bercaw JE (2013) *ACS Catal* 3:2582–2585
23. Li CQ, Wang FF, Lin ZY, Zhang N, Wang J (2016) *Inorg Chim Acta* 453:430–438
24. Chen LD, Huo HL, Wang LB, Ma LL, Jiang Y, Xie JY, Wang J (2019) *Inorg Chim Acta* 491:67–75
25. Wang J, Xie JY, Wang LB, Jiang Y, Zhang N (2019) *Can J Chem* 97:296–302
26. Wang J, Fu ZJ, Zhang N, Li CQ, Shi WG (2017) *J Macromol Sci Part A* 54:465–471
27. Chandran D, Kwak CH, Oh JM, Ahn IY, Ha CS, Kim I (2008) *Catal Lett* 125:27–34
28. Musaeov DG, Froese RDJ, Svensson M, Morokuma K (1997) *J Am Chem Soc* 119:367–374
29. Ahamad T, Alshehri SM (2014) *Adv Polym Technol* 32:586–589

Publisher's Note Springer Nature remains neutral with regard to jurisdictional claims in published maps and institutional affiliations.